10.1109/ULTSYM.2013.0165

Coherent Flow Imaging: A Power Doppler imaging Technique Based on Backscatter Spatial Coherence

Jeremy J. Dahl,[1] Nick Bottenus,[1] Muyinatu A. Lediju Bell,[2,3] and Michael J. Cook[1]
[1]Department of Biomedical Engineering, Duke University, Durham, NC 27708
[2]Department of Radiology, Johns Hopkins University School of Medicine, Baltimore, MD 21287
[3]Department of Computer Science, Johns Hopkins University, Baltimore, MD, 21286
jeremy.dahl@duke.edu

***Abstract*—Power Doppler imaging is a commonly used method for the detection of flow. The direction of flow is lost with power Doppler, but it has greater sensitivity to flow compared to velocity estimation techniques. Power Doppler imaging can be degraded if thermal noise is large or if slowly moving reverberation clutter passes through the wall filter. We have developed a power Doppler imaging technique, based on the same principles as power Doppler, but uses the coherence of backscattered blood signal rather than the complex backscattered signal. This technique, called SLSC power Doppler, is less sensitive to clutter-based signals and thermal noise. We show in simulations, phantom, and *in vivo* experiments that the detected flow demonstrates a smoother, fuller profile and is more robust to the presence of thermal noise. The technique can also utilize fewer ensemble samples to obtain satisfactory detection of flow.**

I. Introduction

Power Doppler imaging is a commonly used method for the detection of flow in many applications. Although direction of flow is lost with power Doppler, it is valued for its greater sensitivity to slow flow compared to color Doppler imaging [1]. Slow flow is compromised in color Doppler imaging because the signal from the slowly moving blood cells is attenuated by the wall filter such that its signal-to-noise ratio is low enough that random noise (e.g. the thermal noise from the system's electronics) can overpower the estimate of the Doppler shift and corrupt the flow estimate. The thermal, or Johnson, noise is not attenuated by the wall filter because it is a white noise process, and appears as a rapidly changing target.

In power Doppler imaging, the output signal is dependent on the energy, or integrated power, of the Doppler signal. If the backscatter of the blood signal is stronger than the background thermal noise, then the blood flow can be differentiated from the thermal noise by means of a threshold. However, if the flow is slow enough such that the blood signal is attenuated by the wall filter, then it is more difficult to differentiate blood from noise. In addition, slowly moving tissue or reverberation clutter that pass through the wall filter can degrade the power Doppler image because it appears similar to slowly moving blood.

Although reverberation clutter and thermal noise impact the Doppler signal differently, the spatial signature of the waveforms are similar. Both sources of noise have relatively low spatial coherence, meaning that the signal recorded by each array element is different. The spatial coherence of backscattered blood signal is like tissue and its backscattered waves are relatively similar over the array elements.

We have developed a flow imaging technique that is similar to power Doppler imaging, but is based on the coherence of backscattered blood signal. This technique utilizes the short-lag spatial coherence (SLSC) method [2] to detect flow signal and differentiate flow from reverberation and thermal noise. We have labeled this class of imaging techniques as coherent flow imaging techniques. Specifically, we call this technique, SLSC power Doppler.

II. Methods

A. SLSC Power Doppler

Conventional power Doppler (PD) relies on an ensemble of radio-frequency (RF) traces to determine if flow is present. A wall, or high-pass, filter is applied to the ensemble of RF traces to attenuate any stationary and slow moving signals. A PD image pixel is generated by summing the power, or squared magnitude, of the complex signal across the filtered ensemble. Loupas et al. [3] proposed a PD calculation based off of their 2D autocorrelator for blood velocity estimation:

$$\mathrm{PD} = \sum_{k=1}^{K} \sum_{n=1}^{N} \left| r(k,n) \right|^2 . \tag{1}$$

Here, $r(k,n)$ is the complex signal, k is the time/depth samples, n is the ensemble sample, and K and N are integer number of samples. The PD calculation proposed by Loupas et al. averages the power calculation over a kernel of length K. In the following, we use the method by Loupas et al. because it more closely resembles the PD images observed on clinical scanners.

SLSC power Doppler (SPD) is based on the same principles as conventional power Doppler imaging. An ensemble of RF traces is required to detect flow, however SPD requires that the individual channel RF signals be stored rather than the fully beamformed RF traces. A wall filter is then applied across the ensemble of each individual channel. The filtered channel signals are used in a conventional SLSC computation, described in Lediju et al. [2], to yield an ensemble of SLSC vectors. Because the backscattered blood signal has the same coherence properties as tissue, the resulting SLSC computation

will yield bright signal from the blood. Thermal noise and any reverberation clutter or other acoustical noise will be suppressed because of their low coherence properties. To created an SPD image pixel, the power of the SLSC vectors is added across the ensemble:

$$\mathrm{SPD} = \sum_{n=1}^{N} V_{slsc}^2(n). \tag{2}$$

Here, V_{slsc} is the SLSC image magnitude, where V_{slsc} is computed over a kernel of size K (see equations 1 and 2 in [4]).

B. Simulations

Simulations of the cross-section of a 2 mm vessel were performed using Field II [5]. Blood signal within the vessel was generated by scatterers 20 dB below the surround tissue scatterers and traveling at a maximum rate of 5 cm/s with a parabolic profile. The scatterers for both the tissue and blood had a density of 10 scatterers per resolution volume. The simulations were performed with a 128-element 7.5 MHz transducer having a pitch of 0.3 mm. The transmitting pulse had a fractional bandwidth of 30% and used an F/2 transmit focused at 2 cm.

Simulated channel signals were acquired for a field-of-view of 5 mm with 0.1 mm beam spacing (for a total of 50 locations). For each location, an ensemble of 15 beams was acquired at a pulse repetition frequency (f_{prf} of 2 kHz. This ensemble was resampled at 666.7 Hz and 400 Hz to yield additional ensemble sizes of 5 and 3, respectively. Thermal noise was incorporated into the simulated channel signals by adding white noise of -40 to 15 dB relative to the blood signal. A 2-tap, highpass, Butterworth IIR filter with projection initialization and a 10 Hz cutoff frequency was used to filter the ensembles.

PD and SPD images were formed over the range of thermal noise and ensemble sizes using a kernel size (K) equivalent to 3λ. The quality of the PD and SPD images was determined using the ratio of the integrated energy within the vessel to the integrated energy of a model vessel. For the discretized images, this is defined as

$$\mathrm{ER} = \frac{\sum\sum_A P(x,z)}{\sum\sum_A M(x,z)}, \tag{3}$$

where $P(x,z)$ is the PD or SPD image in decibels, A is the area of the vessel cross-section, and $M(x,z)$ is a model profile of the power in the vessel. The model can be chosen to match any desired or ideal PD or SPD profile. In the following measurements, the model vessel was chosen to have a flat profile with PD or SPD signal equal to the maximum value within the PD or SPD image, respectively. The integrated energy of $P(x,z)$ and $M(x,z)$ are calculated after shifting the background noise such that its mean is 0 dB.

C. Phantom and In Vivo *Experiments*

Individual channel signals from a flow phantom and *in vivo* thyroid were acquired with an ATL L12-5 transducer and a Verasonics V-1 system (Verasonics, Inc., Redmond, WA). The flow phantom contained a 4 mm vessel, for which a cornstarch and water mixture was used to generate scattering within the vessel. A continuous-flow pump was used to circulate the fluid at 5±0.5 cm/s. The transducer transmitted 6 cycle pulses with a frequency of 5 MHz and an F/2 configuration. 128 channel signals were acquired for 50 locations with an ensemble size of 15 at an f_{prf} of 1 kHz. In addition, a corresponding B-mode image having 129 lateral locations was also acquired. A 2-tap, highpass, Butterworth IIR filter with projection initialization and a 25 Hz cutoff frequency was used to filter the ensemble signals. The ensemble size for the phantom experiment was varied in order to compare the effect of low ensemble sizes on the resulting PD and SPD images. The vessels observed in the *in vivo* thyroid were confirmed by imaging with a Siemens Acuson S2000 ultrasound scanner (Siemens Medical Solutions USA, Inc., Issaquah, WA).

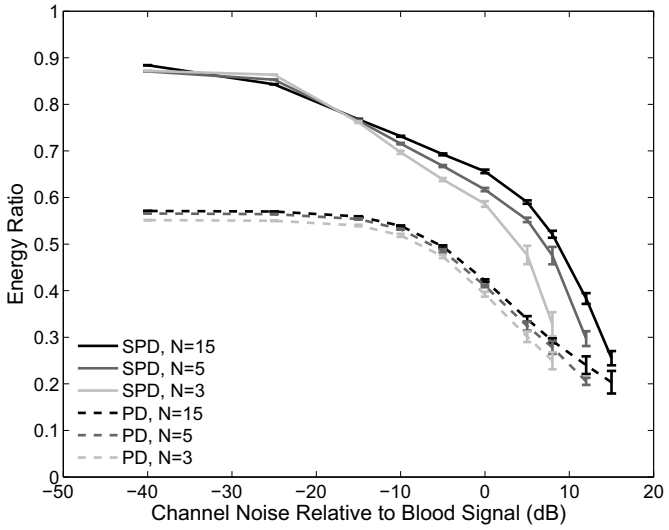

Fig. 1. The energy ratio for PD (dashed lines) and SPD (solid lines) as a function of channel noise for ensemble lengths of 3, 5, and 15. The energy ratio is greater for the SPD images than for the PD images over the range of noise values observed here. Both methods are degraded at large amounts of channel noise.

III. Results and Discussion

Fig. 1 shows the energy ratio calculations for both the simulated PD and SPD images as a function of channel noise. The energy ratios of the SPD images are significantly greater than that of the PD images. The energy ratio indicates that the SPD images demonstrate greater and smoother fill within the vessel region. The energy ratio is not significantly impacted by the ensemble length, however, except at the larger noise values. The energy ratio is improved for the larger ensemble sizes in this region because there is greater correlation of the blood signal across the ensemble (due to the changing f_{prf}). If the blood signal is correlated, then the sum of the blood signal's power increases at a faster rate than the noise. The blood signal is likely not correlated over the entire ensemble, however the additional independent samples of blood signal

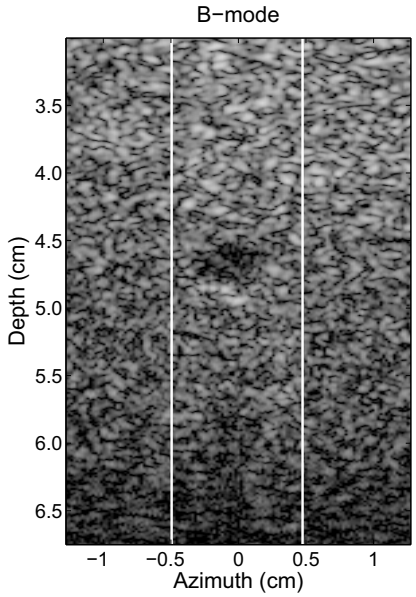

Fig. 2. A B-mode image of the flow phantom showing a 4 mm vessel at approximately 4.75 cm depth.

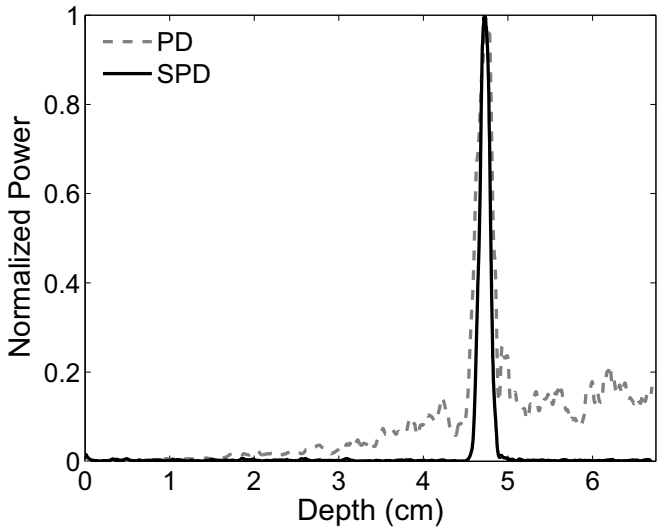

Fig. 3. The PD and SPD profiles of the center image line from the flow phantom. The vessel is observed at 4.75 cm depth. The PD demonstrates thermal noise that increases with increasing depth. The SPD demonstrates an insensitivity to the thermal noise.

will contribute to a smoother profile, much in the way that spatial compounding generates a smoother speckle pattern in B-mode imaging.

Fig. 2 shows a B-mode image of the flow phantom. A cross-section of a 4 mm vessel can be observed at approximately 4.75 cm depth. The vessel does not appear fully anechoic because the cornstarch and water mixture can produce a stronger backscatter than blood, depending on the concentration of the cornstarch. The white lines in this image demarcate the region where ensemble data was acquired for flow detection.

Fig. 3 displays a plot of PD and SPD values through the center of the vessel in the flow phantom, normalized

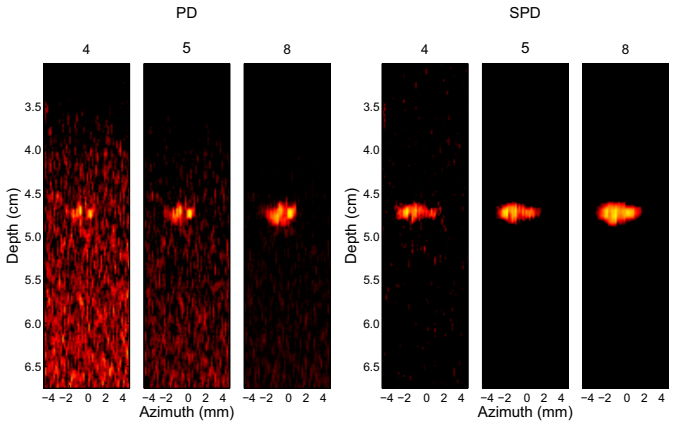

Fig. 4. PD and SPD images as a function of ensemble length. The PD images are grouped on the left, and show poor display of flow for an ensemble size of 4. Flow detection is improved with a larger ensemble. The SPD image (grouped on the right) shows clear flow at an ensemble size of 4. The SPD images show improved detection of the flow with larger ensemble sizes, but mainly in the size of the flow area. All images show 30 dB of dynamic range, except the leftmost image of each group, which shows 34 dB.

by the maximum power value. The PD and SPD images were created with an ensemble size of 15. The center line of the PD image (dashed line) displays a clear indication of flow in a vessel at 4.75 cm. Thermal noise is visible in this plot as the increasing baseline value with depth. The thermal noise increases because the ultrasound signal is attenuated with depth, thereby decreasing the signal-to-noise ratio of the Doppler signal of the deeper signals.

The center line of the SPD image also shows a clear indication of flow in a vessel at 4.75 cm. The SPD image shows no change in the baseline value, however, which remains at approximately 0 throughout depth. The lack of change in this baseline value occurs because the SPD image is insensitive to the thermal noise. The thermal noise is spatially incoherent, and therefore the SLSC processing suppresses its image value.

Fig. 4 displays PD and SPD images of the vessel phantom with ensemble sizes that are smaller than is used conventionally. In this figure, the PD images are grouped on the left, and the SPD images are grouped on the right. All images are logarithmically compressed and show 30 dB of dynamic range, except the images with ensembles of 4, which show 34 dB of dynamic range. The dynamic range limitation is used to threshold the PD signal in order to display expected flow and suppress unwanted thermal noise. In the case of the PD images, the low ensemble size of 4 is incapable of separating the flow signal from the thermal noise. The visual detection of flow improves at an ensemble of 5, although thermal noise is still visible. At an ensemble of 8, a sufficient number of samples are utilized to separate the flow signal and the background noise.

In the SPD images, the flow in the vessel is clearly visible for all ensemble sizes. The area of the flow visualization is slightly smaller for the ensemble size of 4 compared to the other ensemble sizes. The significance of this result is that, assuming computational complexity does not impact the frame

TABLE I
ENERGY RATIO IN FLOW PHANTOM

Ensemble Length	Energy Ratio	
	PD	SPD
4	0.18	0.32
5	0.28	0.50
8	0.40	0.64

rate, power Doppler imaging can be performed at faster frame rates with less degrading effects from noise. The energy ratios of the flow in these images are shown in Tab. I, and show an increasing energy ratio with increasing ensemble size for both PD and SPD imaging. Like the simulated images, the SPD images show a significantly greater energy ratio than the PD images. Neither the PD nor the SPD images display flow over the entire vessel. This is likely a result of clumping of the cornstarch from the slow flow rate.

Fig. 5 compares PD and SPD imaging in an *in vivo* thyroid. The PD and SPD images were formed using an ensemble size of 5 and are overlayed on the B-mode image. The PD and SPD images are showing a vessel within the thyroid that makes a branch or bend at nearly 90 degrees, and was confirmed by observing the vessel with Doppler imaging on a clinical scanner. The vessel is depicted by the bright orange/yellow mark at approximately 2 cm depth. The red mark that produces a "leg" is the corner or branching of the vessel. The display threshold of the PD image has been adjusted such that the PD image shows the vessel approximately the same as in the SPD image. The PD image displays more thermal noise in the lower part of the image, although this is often undetected in clinical systems where the field-of-view is often restricted to box or range. The PD image also shows numerous artifacts at approximately 2.75 cm depth. These artifacts can be reduced by increasing the threshold of the PD image, but this decreases the visualization of the flow, and eliminates the flow detected at the corner or branching vessel.

IV. CONCLUSIONS

We have introduced a flow imaging technique based on the spatial coherence of backscatter from blood. This method, called SLSC power Doppler here, is similar to power Doppler imaging in that the direction of flow is unknown, but is based on the power of the SLSC computation rather than the power of the complex signal. SPD demonstrates suppression of thermal noise, which can obscure slow flow in power Doppler imaging when the noise is of similar amplitude to the blood signal. Our proposed method demonstrates superior performance at low ensemble lengths, which can significantly improve the poor frame rates associated with Doppler imaging techniques. We have demonstrated this technique in the detection of flow in the thyroid, and have shown that it achieves improved reduction of noise artifacts.

ACKNOWLEDGMENTS

This work is supported by the National Institute of Biomedical Imaging and Bioengineering through grants R01-EB013361 and R01-EB015506.

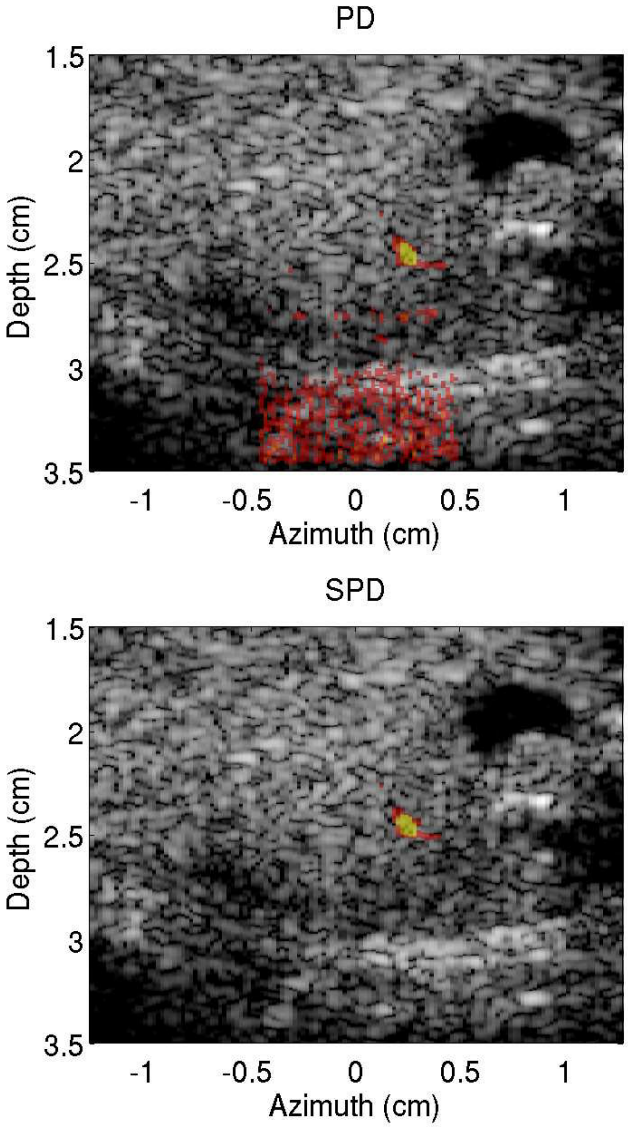

Fig. 5. *In vivo* PD and SPD images in a thyroid. Both images show a vessel with a corner or branch at approximately 2 cm depth. The PD image also displays a greater amount of noise. The threshold of the PD cannot be increase while maintaining the same visualization of the flow as the SPD image. An ensemble size of 5 was used to produce these images.

REFERENCES

[1] J. M. Rubin, R. O. Bude, P. L. Carson, R. L. Bree, and R. S. Adler, "Power Doppler US: A potentially useful alternative to mean frequency-based color Doppler US," *Radiol*, vol. 190, no. 3, pp. 853–856, 1994.

[2] M. Lediju, G. E. Trahey, B. C. Byram, and J. J. Dahl, "Short-lag spatial coherence of backscattered echoes: Imaging characteristics," *IEEE Trans Ultrason Ferroelect Freq Contr*, vol. 58, no. 7, pp. 1377–1388, 2011.

[3] T. Loupas, R. Peterson, and R. Gill, "Experimental evaluation of velocity and power estimation for ultrasound blood flow imaging, by means of a two-dimensional autocorrelation approach," *IEEE Trans Ultrason Ferroelect Freq Contr*, vol. 42, pp. 689–699, 1995.

[4] J. J. Dahl, M. Jakovljevic, G. F. Pinton, and G. E. Trahey, "Harmonic spatial coherence imaging: An ultrasonic imaging method based on backscatter coherence," *IEEE Trans Ultrason Ferroelect Freq Contr*, vol. 59, no. 4, pp. 648–659, 2012.

[5] J. A. Jensen, "Field: A program for simulating ultrasound systems," *Med. Biol. Eng. Comp., col. 10th Nordic-Baltic Conference on Biomedical Imaging*, vol. 4, no. 1, pp. 351–353, 1996.